

# The Vector Probe in Heavy-Ion Reactions

Ralf Rapp§

Cyclotron Institute and Physics Department, Texas A&M University, College Station, Texas 77843-3366, U.S.A.

**Abstract.** We review essential elements in using the  $J^P = 1^-$  channel as a probe for hot and dense matter as produced in (ultra-) relativistic collisions of heavy nuclei. The uniqueness of the vector channel resides in the fact that it directly couples to photons, both real and virtual (dileptons), enabling the study of thermal radiation and in-medium effects on both light ( $\rho, \omega, \phi$ ) and heavy ( $\Psi, \Upsilon$ ) vector mesons. We emphasize the importance of interrelations between photons and dileptons, and characterize relevant energy/mass regimes through connections to QGP emission and chiral symmetry restoration. Based on critical analysis of our current understanding of data from fixed-target energies, we identify open key questions to be addressed.

## 1. Introduction: Towards QGP Discovery

Collisions of heavy nuclei at high energies provide a rich laboratory for studying strongly interacting matter under extreme conditions of (baryon-) density ( $\rho_B$ ) and temperature ( $T$ ). One of the main objectives is the creation and identification of new forms of matter, most notably Quark-Gluon Plasma (QGP), as predicted by the underlying theory, Quantum Chromodynamics (QCD).

As a first step towards this goal, a necessary condition for the investigation of the phase diagram of QCD is an approximate (local) thermalization of the produced matter. Bulk properties of hadron production over a wide range of collision energies have indeed revealed ample evidence for multiple reinteractions, justifying the notion of the production of “matter”. Among the main features that distinguish heavy-ion ( $A$ - $A$ ) collisions from elementary proton-proton ( $p$ - $p$ ) reactions are a strong collective expansion as extracted from hadronic transverse momentum ( $p_t$ ) spectra [1, 2, 3, 4, 5] and (apparent) chemical equilibration inferred from produced hadron species [6, 7], most notably in the strangeness sector. Furthermore, all measurements of dilepton invariant-mass spectra thus far [8, 9, 10, 11, 12] exhibit large excess production in central  $A$ - $A$  collisions over  $p$ - $p$  (or  $p$ - $A$ ) reference spectra. In fact, at energies available at the Super Proton Synchrotron (SPS), theoretical analyses imply [13] that at least 10 generations of  $\pi^+\pi^- \rightarrow e^+e^-$  annihilation are required to reproduce the observed dilepton yields in semi-central  $Pb(158A\text{GeV})$ - $Au$  collisions.

§ email: rapp@comp.tamu.edu

In a second step, one needs to assess thermodynamic state variables (temperature, energy density, pressure) characterizing the produced system. Already with  $Pb$  beams at top SPS energy there have been several indications [14] for temperatures ( $T \geq 200$  MeV) and energy densities ( $\epsilon \geq 3$  GeV/fm<sup>3</sup>) significantly above the critical values obtained from current lattice simulations of finite- $T$  QCD [15]. Recent data from the Relativistic Heavy-Ion Collider (RHIC) at about a factor 10 higher (center-of-mass) collision energy have added spectacular new results on bulk matter properties: (i) the suppression of high- $p_t$  particles (“jet-quenching”) [16], requiring energy densities  $\epsilon \simeq 30$  GeV/fm<sup>3</sup> in the early stages of central  $Au$ - $Au$  collisions; (ii) radial and especially elliptic flow of hadrons at low  $p_t \leq 2$  GeV (comprising more than 95% of the total multiplicity) that are well-described by hydrodynamic simulations [2, 17] favoring formation times of thermalized matter of  $\tau_0 \simeq 0.5$  fm/c implying initial temperatures  $T_0 \simeq 350$  MeV and energy densities quite consistent with (i); (iii) an unexpectedly large baryon-to-meson ratio, as well as an approximate “constituent-quark scaling” of the elliptic flow of all measured hadrons, at intermediate  $p_t \simeq 3 - 6$  GeV, which are both naturally explained by quark coalescence models at the hadronization transition [18, 19, 20].

The third step consists of understanding the nature of the created matter, that is, its microscopic properties including phase changes to establish that a “new” state has indeed been observed. In the present context, this means that one should identify properties of the QGP that go beyond, say, an ordinary electromagnetic plasma. Examples of these include: (1) the  $L^2$  dependence of parton energy loss ( $L$ : path length of traversed matter of a high-energy parton), representing its non-abelian character; (2) the origin of the partonic interactions that allow the system to thermalize on the required short time scales (e.g., resonance states in the QGP as recently found in lattice QCD, or gluon multiplication processes [21] involving 3- and 4-gluon vertices) (3) deconfinement; (4) restoration of the spontaneous breaking of chiral symmetry (SBCS). The last two items are basic features of the high-temperature QCD phase transition that are also well established by lattice simulations [15]. To infer these from ultrarelativistic heavy-ion collisions (URHICs), the vector probe is expected to play a central role. Its uniqueness resides on the fact that it carries the quantum numbers of the photon, which does not undergo strong interactions and thus can carry undistorted information on the hot and dense phases of the fireball, both lightlike ( $\gamma$ ) and timelike (lepton pairs,  $\gamma^* \rightarrow l^+l^-$  with  $l = e, \mu$ ). Whereas photon emission is a suitable observable to assess the temperature of the matter, dileptons encode additional dynamical information through their invariant mass,  $M$ . In particular, in the low-mass region they directly couple to the light vector mesons and thus reflect their mass distribution at the moment of decay, rendering them the prime observable to study mass (de-) generation related to (the restoration of) SBCS. At higher mass, dileptons are a standard tool to measure the abundance of the heavy vector mesons ( $\Psi$  and  $\Upsilon$  families), a systematic study of which is hoped to provide information on deconfinement, see Ref. [22] for a recent overview.

The article is organized as follows: in Sec. 2 we recall basic features of thermal electromagnetic (e.m.) emission in heavy-ion collisions. In Sec. 3 we give a detailed

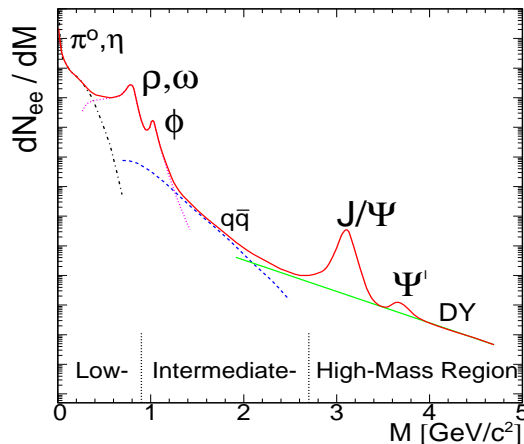


**Figure 1.** Schematic dilepton spectrum in ultrarelativistic heavy-ion collisions.

discussion of the physics potential of thermal dileptons (including comparisons to data), both at low mass in connection with chiral restoration and at intermediate mass in connection with QGP radiation, and summarize their prospects for RHIC. In Sec. 4 we review the current status in the assessment of photon production rates from hot and dense matter, and again put the results into context with measurements at SPS and RHIC. A summary including a list of open questions is given in Sec. 5.

## 2. Four Pillars of Electromagnetic Radiation

Photons and dileptons emerging from heavy-ion collisions can be roughly classified into three categories: (a) “prompt” production associated with primordial  $N$ - $N$  collisions; (b) “radiation” due to (multiple) reinteractions; (c) final state decays of produced hadrons (“cocktail”). A schematic view of a resulting dilepton spectrum is shown in Fig. 1 (adopted from Ref. [23] in slightly modified form). At high masses the prompt yield due to Drell-Yan (DY) annihilation will dominate due to its power-law dependence on  $M$  (rather than exponential characteristic for thermal radiation). On top of the DY continuum the hidden heavy-flavor vector mesons ( $\Psi$ ,  $\Upsilon$ ) are situated; they decay long after strong interactions have ceased (category (c)), with their small number being compensated by large e.m. branching ratios, e.g.  $\Gamma_{e^+e^-}/\Gamma_{tot}=6\%$  (2.5%) for  $J/\psi$  ( $\Upsilon$ ), about  $10^3$  larger than for  $\rho$  or  $\omega$  mesons. The typical window for thermal radiation (category (b)) is below  $M \simeq 3$  GeV. The main background is (i) correlated charm decays,  $D\bar{D} \rightarrow e^+e^-\nu_e\bar{\nu}_e X$ , at intermediate mass,  $1 \text{ GeV} \leq M \leq 3 \text{ GeV}$ , and (ii) Dalitz decays of light mesons ( $\pi^0, \eta, \eta' \rightarrow \gamma e^+e^-$ ,  $\omega \rightarrow \pi^0 e^+e^-$ ) at low mass,  $M \leq 1 \text{ GeV}$ . In the following we will focus on identifying characteristic regimes of thermal radiation.

The response of a strongly interacting system to an e.m. excitation can be quite generally expressed in terms of the pertinent (time-ordered) current correlation function (which, to lowest order in  $\alpha_{em}$ , is just the retarded photon selfenergy) [24, 25],

$$\Pi_{em}(q) = -i \int d^4x e^{iqx} \langle \langle \mathcal{T} j^\mu(x) j^\nu(0) \rangle \rangle, \quad (1)$$

where the brackets denote averaging over the states of the system. E.g., in the case of deep-inelastic scattering the incoming photon is spacelike ( $q^2 < 0$ ), the average is over the nucleon, and the imaginary part of the correlator,  $\text{Im} \Pi_{\text{em}}$ , is directly related to the structure functions of the nucleon. In heavy-ion collisions, one is interested in the *emitted* thermal radiation, which can be either lightlike (real photons,  $q_0 = q$ ) or timelike (dileptons,  $M^2 \equiv q^2 > 0$ ). The respective emission rates are given by

$$q_0 \frac{dN_\gamma}{d^4x d^3q} = -\frac{\alpha_{\text{em}}}{\pi^2} f^B(q_0; T) \text{Im} \Pi_{\text{em}}^T(q_0 = q; \mu_B, T), \quad (2)$$

$$\frac{dN_{e^+e^-}}{d^4x d^4q} = -\frac{\alpha_{\text{em}}^2}{M^2 \pi^3} f^B(q_0; T) \text{Im} \Pi_{\text{em}}(M, q; \mu_B, T), \quad (3)$$

( $f^B$ : thermal Bose distribution). It is very important to note that both photon and dilepton emission are described by the *same* function,  $\text{Im} \Pi_{\text{em}}||$ . Theoretical models for photon and dilepton spectra in URHICs ought to satisfy this consistency constraint.

Eqs. (2) and (3) are to leading order in the e.m. coupling  $\alpha_{\text{em}}$ , but exact in the strong interactions encoded in  $\Pi_{\text{em}}$ . The photon rate is  $\mathcal{O}(\alpha_{\text{em}})$ , while it is  $\mathcal{O}(\alpha_{\text{em}}^2)$  for dileptons. From the experimental point of view this appears to be an advantage for photon production, but from the theoretical point of view it is not. This is so because, to leading order in the *strong* interactions, the photon rate is  $\mathcal{O}(\alpha_s)$  whereas the dilepton rate is  $\mathcal{O}(1)$ , and thus, at sufficiently high mass, under better theoretical control. Indeed, in the vacuum,  $\text{Im} \Pi_{\text{em}}$  is nonzero only for  $M^2 > 4m_\pi^2$ , and can be determined from  $e^+e^-$  annihilation into hadrons. At low masses,  $M \leq 1$  GeV,  $j_{\text{em}}^\mu$  can be rather accurately saturated by the light vector mesons  $\rho$ ,  $\omega$ , and  $\phi$ , whereas at high masses it becomes amenable to a perturbative description in terms of quark fields, resulting in

$$\text{Im} \Pi_{\text{em}}^{\text{vac}}(M) = \begin{cases} \sum_{V=\rho,\omega,\phi} \left( \frac{m_V^2}{g_V} \right)^2 \text{Im} D_V(M) & , M \leq M_{\text{dual}} \\ -\frac{M^2}{12\pi} \left( 1 + \frac{\alpha_s(M)}{\pi} + \dots \right) N_c \sum_{q=u,d,s} (e_q)^2 & , M \geq M_{\text{dual}} . \end{cases} \quad (4)$$

From the inclusive cross section for  $e^+e^- \rightarrow \text{hadrons}$  one finds  $M_{\text{dual}} \simeq 1.5$  GeV.

For time-integrated yields from a heavy-ion collision it is useful to estimate which temperature regime is predominately probed at given  $M$  (or  $q_0$ ), cf. also [27]. Let us first focus on the dilepton case and perform spatial integrations over Eq. (3) to obtain

$$\begin{aligned} \frac{dN_{ee}}{dM d\tau} &= \frac{M}{q_0} \int d^3x d^3q \frac{dN_{ee}}{d^4x d^4q} \\ &\simeq \text{const} V_{FB}(T) \frac{\text{Im} \Pi_{\text{em}}(M; T)}{M} \int \frac{d^3q}{q_0} e^{-q_0/T} \\ &\simeq \text{const} V_{FB}(T) \frac{\text{Im} \Pi_{\text{em}}(M; T)}{M^2} e^{-M/T} (MT)^{3/2} \end{aligned} \quad (5)$$

For simplicity, we have employed a uniform 3-volume as well as a nonrelativistic approximation,  $M \gg T$ . To infer the temperature dependence of the volume and

|| In fact,  $\Pi_{\text{em}}$  also governs charge fluctuations via the e.m. susceptibility, obtained from the static spacelike limit,  $\chi_{\text{em}} = \Pi_{\text{em}}(q_0=0, q \rightarrow 0)$ , cf. Ref. [26] for a recent discussion of this point.

proper time, we assume isentropic expansion, i.e., the total entropy  $S=sV_{FB}$  to be conserved. Then  $V_{FB}(T) \propto T^{-n}$  with  $n=3$  for an ultrarelativistic ideal gas, (e.g.,  $s = d_{QG}(4\pi^2/90)T^3$  for massless quarks and gluons with degeneracy  $d_{QG}$ ), whereas  $n \simeq 4-5$  for a resonance hadron gas. The dependence of proper time on  $T$ ,  $\tau \propto T^{-k}$  (or  $d\tau \propto T^{-k-1}dT$ ), is sensitive to the expansion dynamics: for the purely longitudinal (1-D Bjorken) case, appropriate for early phases in URHICs, one has  $s_0\tau_0 = s\tau$  and thus  $\tau \propto T^{-n}$ ; in the later stages the expansion is closer to 3-D, implying  $\tau \propto T^{-n/3}$ . Collecting the various powers one finds

$$\begin{aligned} \frac{dN_{ee}}{dMdT} &\propto T^{-n-k-1} e^{-M/T} (MT)^{3/2} \frac{\text{Im}\Pi_{\text{em}}(M;T)}{M^2} \\ &\propto \text{Im}\Pi_{\text{em}}(M;T) e^{-M/T} T^{-5.5}, \end{aligned} \quad (6)$$

approximately holding for both early and later phases. To find the regime of maximal emission one simply takes the temperature derivative.

At large  $M$ , where  $\text{Im}\Pi_{\text{em}}(M;T)$  is only weakly dependent on  $T$  (corrections are of order  $\mathcal{O}(\alpha_s T^2/M^2)$ ), one finds  $T_{max} \simeq M/5.5$ , e.g., at  $M = 2$  GeV one has  $T_{max} = 360$  MeV, well inside the QGP. In fact, this estimate has to be taken with care, as the function  $f(z) = e^{-1/z}/z^{5.5}$  ( $z \equiv T/M$ ) has a substantial tail towards large  $z$ . Calculating the yield as a function of initial temperature  $T_0$ ,  $Y(z_0) \equiv \int_0^{z_0} f(z)dz$ , it turns out that 2/3 (90%) of the limiting yield,  $Y(z_0=\infty)$ , is reached only for  $z_0 \simeq 0.3$  (0.5). For  $M=2$  GeV this implies  $T_0 \simeq 600$  MeV (1 GeV), well above  $T_{max}$ . In practice this means: (i) at both RHIC and LHC dilepton radiation in the intermediate mass region is dominated by QGP emission, (ii) whereas at RHIC the yield is sensitive to the initial conditions, it could be close to its maximal value at LHC.

An interesting opportunity could arise in the  $M \simeq 1.5$  GeV region through resonance states in the QGP as predicted by recent lattice QCD calculations [28]. If the  $\rho$  meson survives, a dilepton excess could occur [29] around its expected mass,  $m_\rho \simeq 2m_q^{th} \sim 2gT$ .

In the low-mass region,  $M \leq 1$  GeV, the situation is more complicated since the e.m. correlator is directly proportional to the vector-meson spectral functions, which, via their in-medium modifications, induce further temperature- and density-dependencies (see also Sec. 3.2 below). Model calculations [13] suggest that the largest contribution to the thermal yield below the free  $\rho/\omega$  mass originates from the *hadronic* phase close to  $T_c$ , thus providing favorable conditions for probing chiral symmetry restoration.

Arguments similar to the dilepton case apply to photon radiation, where the measured spectra are usually quoted as an invariant yield  $q_0 dN_\gamma/d^3q = dN_\gamma/dy d^2q_t$  versus transverse momentum  $q_t$  in a given range of rapidity,  $y$ . The temperature profile of the yield can be inferred as above, with 2 modifications: (i) there is no integration over  $q$ , so no factor  $(MT)^{3/2}$  arises; (ii) even to lowest order in  $\alpha_s$ ,  $\text{Im}\Pi_{\text{em}}(q_0=q)$  carries a leading temperature dependence, e.g.  $\propto T^2$  in perturbative QCD calculations [30, 31, 32, 33, 34]. Thus, at sufficiently high energies and for 1-D expansion one has

$$\frac{dN_\gamma}{dy d^2q_t} \propto T^{-n-k-1} e^{-q_0/T} \text{Im}\Pi_{\text{em}}(q_0=q) \propto T^{-5} e^{-q_0/T}, \quad (7)$$

	Low Mass/Energy	Intermediate Mass/Energy
Dileptons	in-medium $\rho$ , $\omega$ , $\phi$ Chiral Symmetry Restoration?	continuum emission ( $q\bar{q} \rightarrow ee$ ) leading order $\mathcal{O}(\alpha_{\text{em}}^2)$ QGP Radiation?
Photons	hadron decays/scattering $a_1 \rightarrow \pi\gamma$ , $\pi\rho \rightarrow \pi\gamma$ Medium Effects?	continuum emission leading order $\mathcal{O}(\alpha_{\text{em}}\alpha_s)$ QGP Radiation?

**Table 1.** The four pillars of thermal emission of electromagnetic radiation.

which is almost identical to dileptons, i.e., photon radiation at energies  $q_0 \geq 2$  GeV is also a sensitive probe of the early (QGP) phases.

At low energies,  $q_0 \leq 1$  GeV, photon spectra are dominated by hadronic emission, which is again difficult to quantify due to the  $T$ -dependence of the e.m. correlator. Another subtlety for photons is that, unlike the dilepton invariant mass, the photon transverse momentum is Lorentz-variant and therefore sensitive to transverse flow velocities, entailing blue-shifts in the spectrum (more pronounced for the later stages).

The main features of the above discussion are summarized in Table 1.

### 3. Thermal Dileptons

#### 3.1. Chiral Symmetry

Let us recollect some elements of chiral symmetry, its breaking and restoration, which are relevant for the subsequent discussion.

For the two lightest quark flavors ( $u$  and  $d$ ) the QCD Lagrangian

$$\mathcal{L} = \bar{q}(i \not{D} - \hat{m}_q)q - \frac{1}{4}(G_a^{\mu\nu})^2 \quad (8)$$

possesses a  $SU(2)_L \times SU(2)_R$  (“chiral”) symmetry (a combination of invariance in isospin and left- and right-handed quark-fields). It is only slightly broken explicitly by small *current* quark masses  $m_{u,d} \simeq 5 - 10$  MeV (which enter the matrix  $\hat{m}_q = \text{diag}(m_u, m_d)$  and originate from electroweak interactions). A much more dramatic phenomenon is the *spontaneous* breaking of chiral symmetry (SBCS), which is induced by a strong attraction in the scalar  $q\bar{q}$  channel leading to the formation of a quark condensate,  $\langle 0|\bar{q}q|0\rangle \simeq -(250\text{MeV})^3$ , filling the QCD vacuum. Although the condensate is not an observable, it manifests itself in (hadronic) excitations of the vacuum, e.g. (i) at the quark level, an energy gap  $\Delta_{\bar{q}q} \equiv m_q^* \propto \langle \bar{q}q \rangle$  generates a *constituent* quark mass  $m_q^* \simeq 350$  MeV which constitutes the major portion of the visible mass in the universe; (ii) there appear 3 (almost) massless (quasi-) Goldstone bosons, the pions ( $m_\pi^2 \propto m_q$ ); (iii) a substantial mass difference of  $\Delta M \simeq 0.5$  GeV splits hadronic states within chiral multiplets (which in a chirally symmetric vacuum state would be degenerate). For the light vector mesons in the 2-flavor sector, the  $\omega(782)$  turns out to be a chiral singlet,

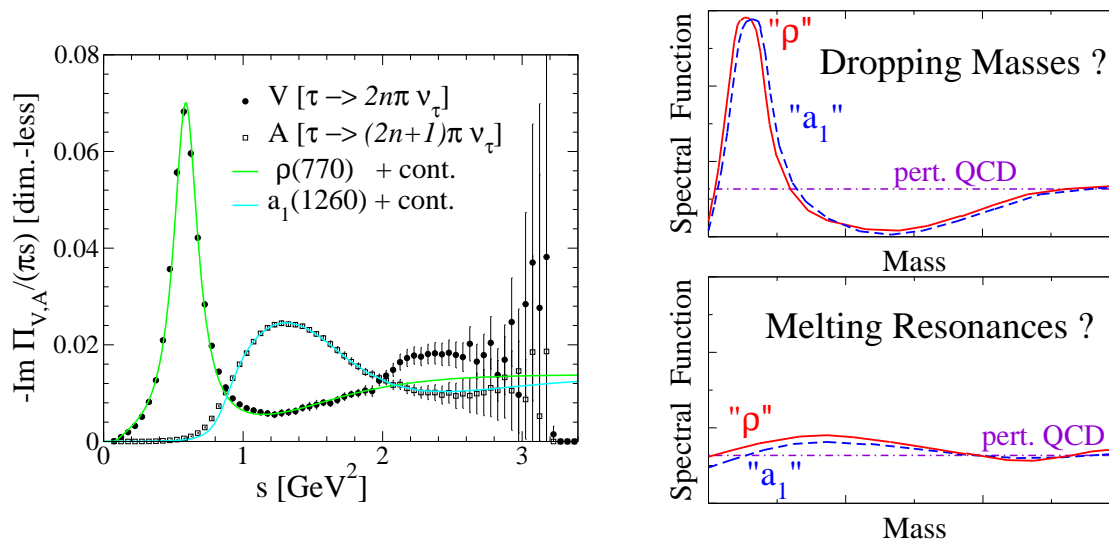


**Figure 2.** Left panel: vector and axialvector spectral functions as measured in hadronic  $\tau$  decays [36] with model fits using vacuum  $\rho$  and  $a_1$  spectral functions plus perturbative continua [37]; right panel: two possible scenarios for chiral symmetry restoration in matter.

whereas the chiral partner of the  $\rho$  meson is usually identified with the  $a_1(1260)$ ¶. The respective vector ( $V$ ) and axialvector ( $A$ ) spectral functions have been measured in  $\tau$  decays, cf. left panel of Fig. 2. Albeit limited by the  $\tau$  mass,  $m_\tau^2=3.16 \text{ GeV}^2$ , the spectra indicate the approach to the perturbative limit (and each other) at large  $s=q^2$ ,  $-\text{Im}\Pi_{\text{em,pert}}^{I=1}/(\pi s)=\frac{N_c}{12\pi^2}\times\frac{1}{2}$ , cf. Eq. (4) (the factor of  $\frac{1}{2}$  counts the isospin  $I=1$  part of the correlator, with the remaining  $\frac{1}{18}$  supplemented by the  $I=0$   $\omega(782)$ ), affirming that SBCS is a low-energy phenomenon. The connection to SBCS can be quantified by the 2. Weinberg sum rule [38],

$$f_\pi^2 = - \int \frac{ds}{\pi s} [\text{Im}\Pi_V(s) - \text{Im}\Pi_A(s)] , \quad (9)$$

relating the pion decay constant  $f_\pi$ , one of the order parameters of SBCS (the ‘‘pole strength’’ of the Goldstone mode), to the (integrated) difference of  $V$  and  $A$  spectral functions. Note that it is not only the mass, but the entire spectral shape that matters. Importantly, Eq. (9) remains valid at finite temperature [39], replacing  $s \rightarrow q_0^2$  at fixed  $q$ .

Towards the critical temperature ( $T_c$ ), chiral symmetry restoration requires the  $V$  and  $A$  spectral functions to (approximately) degenerate (lattice calculations show that  $\langle \bar{q}q \rangle(T)/\langle \bar{q}q \rangle(0)$  drops rather rapidly around  $T_c$  down to  $\sim 10\text{-}15\%$  slightly above  $T_c$ ). *How* this is realized, is one of the main questions in strong interactions, shedding light on the question of mass generation. Two of the infinitely many possibilities are illustrated in Fig. 2 (right panel).

¶ In recent work by Harada *et al* [35] the ‘‘vector manifestation’’ of chiral symmetry has been suggested in which the chiral partner of the (longitudinal component of the)  $\rho$  meson is identified with the pion.

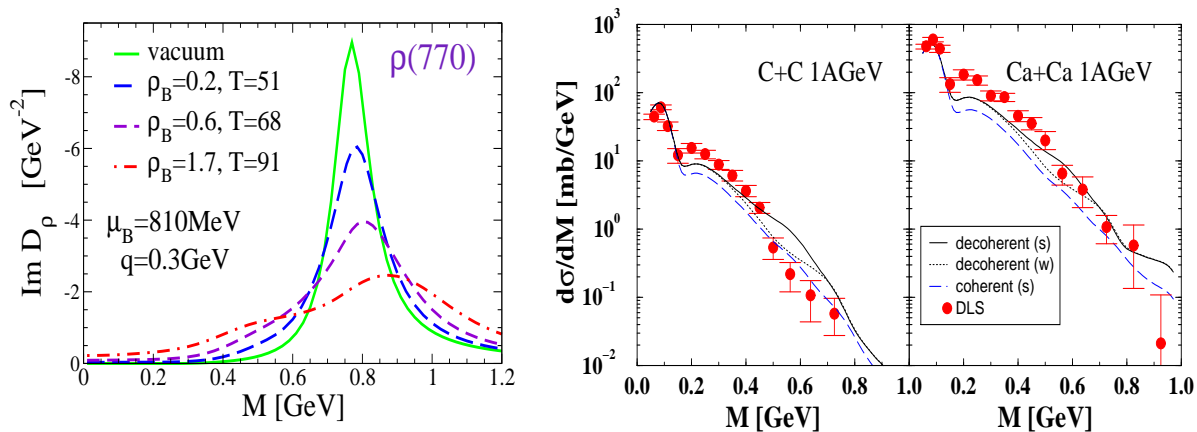


**Figure 3.** Left panel:  $\rho$  spectral function under conditions resembling heavy-ion collisions at BEVALAC/SIS energies [45]. Right panel: transport calculations [47] of  $e^+e^-$  cross sections in 1 AGeV  $C+C$  and  $Ca+Ca$  collisions employing broadened  $\rho$  and  $\omega$  spectral functions with (long-dashed line) and without (solid and dotted lines) coherence effects in baryon resonance decays, compared to DLS data [8].

### 3.2. Low-Mass Dileptons

Nature is kind to us in that it rather directly lets us probe the isospin-1 part of the vector correlator: in the thermal dilepton rate, Eq. (4), the isovector (“ $\rho$ ”) channel dominates over the isoscalar (“ $\omega$ ”) by a factor  $\Gamma_{\rho \rightarrow ee} / \Gamma_{\omega \rightarrow ee} = g_\omega^2 / g_\rho^2 \simeq 10$ . Consequently, vigorous theoretical efforts have been devoted to assess medium modifications of the  $\rho$  meson (see Ref. [13] for a review), especially after it became clear that CERES data [9] are incompatible with a vacuum  $\rho$ -meson line shape.

In hadronic many-body approaches one evaluates an in-medium  $\rho$  propagator,

$$D_\rho(M, q; \mu_B, T) = \left[ M^2 - (m_\rho^{(0)})^2 - \Sigma_{\rho\pi\pi} - \Sigma_{\rho B} - \Sigma_{\rho M} \right]^{-1}, \quad (10)$$

in terms of selfenergies arising from direct interactions with surrounding baryons ( $\Sigma_{\rho B}$ ) and mesons ( $\Sigma_{\rho M}$ ), as well as from (in-medium)  $\pi\pi$  loops ( $\Sigma_{\rho\pi\pi}$ ). Underlying hadronic Lagrangians are constrained by free decay widths and/or scattering data (including photoabsorption on nucleons and nuclei [40]), and resulting spectral functions in nuclear matter have been found to satisfy QCD sum rules [41, 42]. The rather generic results of such calculations are (i) a substantial broadening of the  $\rho$  spectral function, with little mass shift (real parts of various contributions to  $\Sigma_\rho$  tend to cancel, whereas imaginary parts strictly add up), (ii) the prevalence of baryonic over mesonic effects (also confirmed in chiral expansion schemes [43]), cf. Fig. 3 (left panel) for an example.

The “dropping  $\rho$ -mass” scenario, which was originally suggested within a mean-field approach exploiting scale invariance of (classical) QCD [44], has received renewed support in the “vector manifestation” of chiral symmetry [35] (see footnote above): at  $T_c$  the longitudinal component of the  $\rho$  (rather than the scalar “ $\sigma$ ” field) degenerates with the pion, forcing its bare mass  $m_\rho^{(0)}$  to (approximately) zero.

Concerning applications to heavy-ion collisions, let us start from low energies. Current calculations cannot account for the large enhancement observed by DLS in



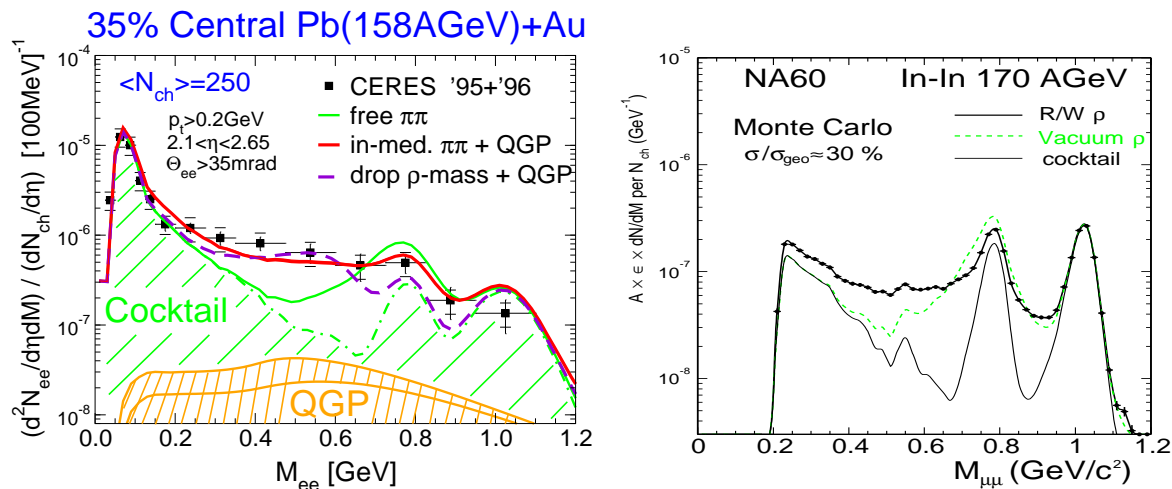


**Figure 4.** Left panel:  $e^+e^-$  spectra in  $Pb(158\text{AGeV})+Au$  [9] compared to thermal fireball calculations [49, 37] using free (dotted line), in-medium many-body (solid line) and dropping-mass  $\rho$ -spectral functions. Right panel: Simulations of  $\mu^+\mu^-$  spectra [52] as expected to be measured by NA60 in  $In(170\text{AGeV})+In$  [51] (solid curve: hadron decays, dashed curve and full circles: using free and in-medium [49]  $\text{Im}D_\rho$ , respectively).

$C+C$  and  $Ca+Ca$  collisions at 1 AGeV, neither with many-body spectral functions [45] nor with a dropping  $\rho$ -mass, nor with both [46]. More recently it has been pointed out [47] that a decoherence of the lepton-pair producing sources (i.e. virtual vector mesons implemented with destructive phase factors in elementary  $p-p$  collisions) in dense matter can lead to some additional (albeit not enough) enhancement in the DLS spectra, cf. right panel of Fig. 3. At the same time, optimal (fitted) values for in-medium  $\rho$  and  $\omega$  widths have been extracted [47] which are consistent with the many-body calculations discussed above (left panel of Fig. 3). New precision data in this energy regime are expected soon from the HADES experiment [48] at SIS (GSI).

At SPS energies, theoretical models compare more favorable with existing data, see left panel of Fig. 4. However, at this point both hadronic many-body calculations and a dropping  $\rho$ -mass scenario are compatible with the CERES data [9]. The prevalence of baryon-driven medium effects predicted within the many-body approach [50, 49] has recently been confirmed experimentally by a relatively larger excess observed at lower SPS energy of 40 AGeV [12]. Also note that the QGP contribution to the in-medium yield in the low-mass region is at the 10-15% level. Very promising new data are expected from the NA60 experiment at SPS [51]. The larger available data sample from muon pairs combined with an improved low- $q_t$  capability due to a new vertex detector leads to simulation results [52] indicating excellent resolution and statistics, cf. right panel of Fig. 4. In particular  $\omega$ - and  $\phi$ -peaks will be clearly discernible.

In-medium effects on the  $\omega$  meson [41, 53, 54, 55, 56] are expected to be of similar magnitude as for the  $\rho$ , but the  $\phi$  seems to be more robust (which is probably related to the OZI rule suppressing resonant  $\phi$ -N interactions). Nevertheless, there are interesting issues related to the  $\phi$ -meson, e.g. comparisons of its line shape and yield in  $l^+l^-$  vs.

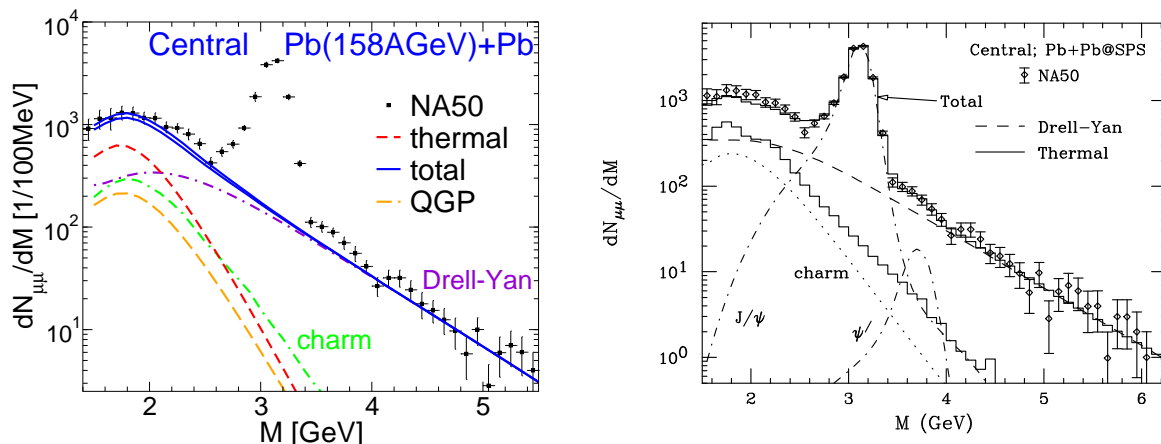


**Figure 5.**  $\mu^+\mu^-$  spectra measured by NA50 [11] at the SPS compared to theoretical calculations addressing the excess at intermediate masses,  $1.5 \text{ GeV} \leq M_{\mu\mu} \leq 3 \text{ GeV}$ . Left panel: thermal fireball model [58]; right panel: hydrodynamical model [59].

$K^+K^-$  decay channels, see, e.g., Haglin’s talk at this meeting [57].

### 3.3. Intermediate Mass Dileptons

The main issue at dilepton masses above  $\sim 1.5 \text{ GeV}$  is how the QGP signal compares to competing sources, i.e., Drell-Yan annihilation, hadron gas radiation and correlated open-charm decays. Assuming the emission rate to be given by its perturbative form, Eq. (4), the key ingredient is the space-time evolution of the system. In Fig. 5 a hydrodynamic [59] (right panel) and a thermal fireball calculation [58]<sup>+</sup> (left panel) are compared to NA50 data [11] from central  $Pb(158 \text{ AGeV})-Pb$  collisions at SPS. Whereas in Ref. [58] 2/3 of the thermal yield originates from the hadronic phase (1/3 from a QGP with uniform initial temperature of  $T_0 \simeq 210 \text{ MeV}$ ), Ref. [59] assigns a larger fraction to the QGP (induced by initial temperatures  $T_0 \simeq 300 \text{ MeV}$ ). This difference deserves further investigation; two possible reasons are: (i) the hydrodynamic equations are solved assuming boost invariance which is not present in the fireball parametrization, (ii) the hadronic equation of state is in chemical equilibrium in the hydro-calculation while in the fireball expansion meson-chemical potentials are introduced to conserve the hadron ratios after chemical freezeout. Nevertheless, in either case the thermal yield accounts for the observed excess, which, in particular, leaves little room for an “anomalous enhancement” of open-charm production. Also in this context, further experimental scrutiny is expected from upcoming NA60 data [51].

### 3.4. Prospects for RHIC and Future Developments

At RHIC, both low- and intermediate-mass dileptons will be measured by PHENIX [60]. For medium effects on the low-mass vector mesons it is important to realize [53] that the relevant quantity is not the *net* baryon density (which is small at RHIC), but the *total*,

<sup>+</sup> The same evolution is underlying the results shown in Figs. 4 and 7.

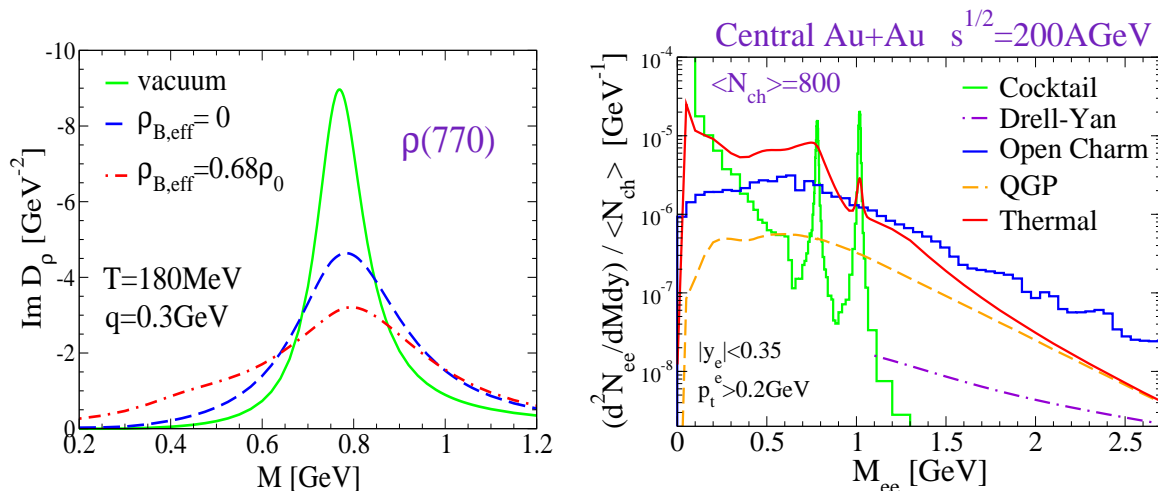


**Figure 6.** Left panel:  $\rho$ -meson spectral function in vacuum and under RHIC conditions with (dash-dotted line) and without (dashed line) the effects of anti-baryons [53]. Right panel:  $e^+e^-$  spectra at RHIC; histograms: final-state decays of open-charm and light hadrons [62], solid line: combined thermal yield [53] from hadronic matter (using in-medium vector spectral functions) and QGP (dashed line).

$\varrho_{tot} \equiv \varrho_B + \varrho_{\bar{B}}$  (due to  $CP$ -invariance of strong interactions mesons interact equally with baryons and antibaryons). The combined effect of  $B$  and  $\bar{B}$  on the  $\rho$  spectral function at RHIC is indeed substantial, especially at masses below 0.5 GeV, see Fig. 6 (left panel). Quantitatively also important is the conservation of the  $\bar{B}$ -number in the hadronic evolution subsequent to chemical freezeout [61], which is necessary to maintain the observed hadron ratios (and implies a significant  $B+\bar{B}$  density, and thus stronger medium effects, in the later phases). The ensuing (space-time integrated) thermal dilepton spectrum [53] in central  $Au$ - $Au$  collisions (right panel of Fig. 6) exhibits an essentially melted  $\rho$  resonance, while the  $\omega$  and  $\phi$  resonance regions are mostly populated by the hadronic cocktail [62] (i.e., decays after freezeout).

At intermediate masses,  $M_{ee} > 1.5$  GeV, the thermal yield is dominated by QGP radiation. However, the increase in  $c\bar{c}$  production by about a factor  $\sim 100$  over the yield at SPS renders correlated charm decays [62] the prevalent source, at least if their transverse-momentum distributions are taken from production in hard (primordial)  $N$ - $N$  collisions. If, on the other hand,  $c$ -quarks undergo re-interactions (e.g. within the QGP), the isotropization of their momentum distributions is likely to lead to a softening of the pertinent dilepton invariant-mass spectra, possibly re-opening the window on QGP radiation. Due to transverse-flow effects on the relatively heavy  $c$ -quarks this softening will be less pronounced than originally expected [63].

Future developments from the theoretical side will have to address the question of in-medium  $a_1$  spectral functions, to strengthen the connections to chiral symmetry restoration (it may even be possible to study medium modifications the  $a_1$  experimentally via  $\pi\gamma$  invariant-mass spectra). The importance of baryon effects in the  $\rho$  and  $\omega$  propagators calls for a more detailed analysis of baryon properties themselves

in hot hadronic matter, see van Hees' talk at this meeting [64].

Furthermore, hadronic models be can used to calculate Euclidean correlation functions via a straightforward folding with a thermal factor,

$$\Pi_\alpha(\tau, q; T) = \int_0^\infty dq_0 \operatorname{Im}\Pi_\alpha(q_0, q) \frac{\cosh[q_0(\tau - 1/2T)]}{\sinh[q_0/2T]} \quad (11)$$

( $\alpha = V, A$ ), which provides a direct means of comparison to lattice “data” for  $\Pi_\alpha(\tau)$ , rather than having to apply an inverse integral transform to the latter.

#### 4. Thermal Photons

Recent progress in assessing thermal photon rates from hot and dense matter has been reviewed by several authors [65, 66, 67, 68]. As emphasized in Sec. 2, one of the difficulties is that the leading term in the thermal photon rate is to nontrivial order in  $\alpha_s$ , implying the absence of a vacuum baseline for  $\operatorname{Im}\Pi_{\text{em}}$  at the photon point.

For the QGP, it has been realized [69] that early perturbative (tree-level) calculations [30, 31, 32, 33] for  $q\bar{q} \rightarrow g\gamma$  and  $qg \rightarrow q\gamma$  receive contributions at the same (leading) order from Bremsstrahlung's processes involving  $t$ -channel gluon exchange, due to forward infrared singularities in the latter. The required resummation to obtain the full result has been accomplished in Ref. [34]; the pertinent rates exhibits a factor 2-3 enhancement over the early results, cf. Fig. 7 (left panel). For hot hadronic matter,  $t$ -channel meson exchange is expected to be the predominant source of high-energy photons, most notably  $\pi$  exchange in  $\pi\rho \rightarrow \pi\gamma$ . There has been some controversy in the literature concerning the role of the  $a_1$   $s$ -channel contribution (or, equivalently,  $a_1$  decays): on general grounds, this source should be suppressed at high energy due to an extra  $1/s$ -dependence in the  $a_1$  propagator, which is even more pronounced if hadronic vertex form factors are included based on a  $\chi^2$ -fit to the  $a_1$  hadronic and radiative decay branchings in vacuum [70]. Baryonic sources have recently been assessed in Refs. [71, 70]. In Ref. [70], previous calculations of the e.m. correlator in the timelike regime [49] were carried to the photon point, thus establishing consistency with in-medium dilepton rates. One finds that the baryonic effects in the photon rate dominate hadronic emission for energies  $\sim 0.2$ -1 GeV (cf. left panel of Fig. 7). Another, somewhat surprising, result of Ref. [70] is that  $\omega$   $t$ -channel exchange in  $\pi\rho \rightarrow \pi\gamma$  becomes the dominant reaction at high energies (due to the large  $\pi\rho\omega$  coupling constant). Reactions involving strangeness were found to contribute at the  $\sim 25\%$  level.

A comparison between (top-down extrapolated) LO-QGP and (bottom-up extrapolated) total hadronic rates in the vicinity of  $T_c$  indicates that both are very similar (this has also been noticed for dilepton rates [49, 37]). If not a coincidence, it could be related to a kind of quark-hadron duality, reminiscent to inclusive electron scattering [72].

Turning to heavy-ion data, WA98 [73] found a significant excess over  $p$ - $p$  extrapolated primordial production in central  $Pb(158A\text{GeV})+Pb$  at SPS. The excess can be nicely explained by thermal (QGP-) radiation with (average) initial temperatures

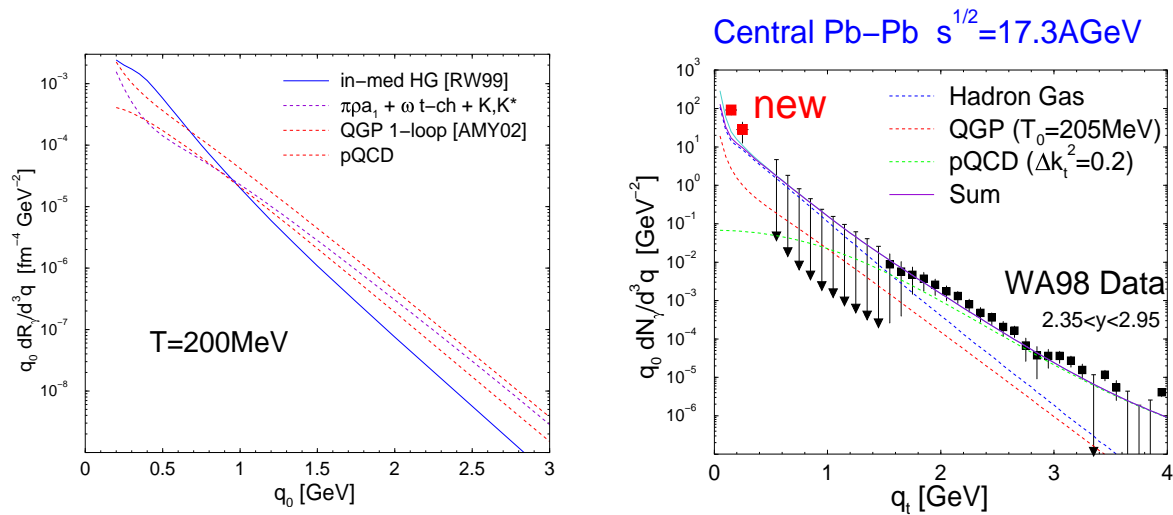


**Figure 7.** Left panel: Thermal photon rates from hot hadronic matter [70] (solid and long-dashed line) and QGP (short-dashed line: tree-level pQCD [32, 33], dashed-dotted line: complete leading order [34]). Right panel: WA98 data [73, 75] compared to thermal fireball calculations [70]; the upper solid line at low  $q_t$  additionally includes Bremsstrahlung from  $S$ -wave  $\pi\pi$  scattering [76].

$\bar{T}_0 \geq 250 \text{ MeV}$  [74]. However, if one allows for a moderate Cronin effect in the primordial pQCD contribution, the latter essentially exhausts the yield above  $q_t \simeq 2 \text{ GeV}$ , and the QGP contribution becomes subdominant to the hadronic one [70] (cf. right panel of Fig. 7), a hierarchy quite similar to the NA50 dileptons (right panel of Fig. 5). New data at low  $q_t$  indicate significant excess over current calculations [70]. The inclusion of soft  $\pi\pi$  Bremsstrahlung slightly improves the situation [76] but additional effects seem to be required, e.g. a softening of the “ $\sigma$ ”-meson or medium-modified  $\Delta$  decays [64].

Preliminary data on direct photons in central  $Au-Au$  at RHIC by PHENIX [77] show a substantial enhancement over hard production at high  $q_t$ . The signal is not yet sensitive to predicted thermal yields [78, 70].

## 5. Conclusions

Electromagnetic radiation from hot and dense QCD matter constitutes a valuable source of information on both its thermal and microscopic properties, in particular (a) on early temperatures at masses/energies  $\geq 1.5 \text{ GeV}$ , and (b) on hadronic in-medium effects, with a potential to study chiral restoration, at  $M, q_0 \leq 1 \text{ GeV}$ . Microscopically consistent calculations of the e.m. correlator have been able to explain photon and dilepton spectra at the SPS in terms of thermal radiation with fair success. Among the questions that have not been answered to date are:

- Is there a deeper reason for the agreement between in-medium hadronic and (resummed) pQCD calculations for both dilepton and photon rates around  $T_c$ ?
- How is chiral restoration realized in the vector-axialvector channel? What is the role of baryons? Can one devise observables to distinguish different scenarios?

- If confirmed, what are possible explanations for the large enhancement of low-energy photons observed by WA98?
- If confirmed by HADES, what is the origin of the thus far unexplained low-mass dilepton enhancement at the BEVALAC?

With the anticipated wealth of upcoming (precision) data over a wide range of energies (SIS, SPS, RHIC and LHC), the combination of theory and phenomenology ought to provide answers.

### Acknowledgment

I thank the workshop organizers for the invitation to a very informative meeting. It is a pleasure to acknowledge my collaborators on the presented topics, C. Gale, L. Grandchamp, E. Greco, C.M. Ko, S. Turbide, H. van Hees and J. Wambach.

### References

- [1] Hung C M and Shuryak E V 1998 *Phys. Rev. C* **57** 1891
- [2] Kolb P F and Heinz U 2003 in Hwa R C and Wang X-N (eds.) *et al Quark gluon plasma* 634, and arXiv:nucl-th/0305084
- [3] Bass S A *et al* 1998 *Prog. Part. Nucl. Phys.* **41** 225
- [4] Bratkovskaya E L *et al* 2000 *Nucl. Phys. A* **675** 661
- [5] Zhang B, Ko C M, Li B-A and Lin Z-W 2000 *Phys. Rev. C* **61** 067901
- [6] Becattini F *et al* 2001 *Phys. Rev. C* **64** 024901
- [7] Braun-Munzinger P, Redlich K and Stachel J 2003 in Hwa R C and Wang X-N (eds.) *et al Quark gluon plasma* 491, arXiv:nucl-th/0304013
- [8] DLS Collaboration (Porter R J *et al* ) 1997 *Phys. Rev. Lett.* **79** 1229
- [9] CERES/NA45 Collaboration (Agakichiev G *et al* ) 1998 *Phys. Lett. B* **422** 405; 2003 *Nucl. Phys. A* **715** 262
- [10] HELIOS-3 Collaboration (Angelis A L S *et al* ) 2000 *Eur. Phys. J. C* **13** 433
- [11] NA50 Collaboration (Abreu M C *et al* ) 2000 *Eur. Phys. J. C* **14** 443
- [12] CERES/NA45 Collaboration (Adamova D *et al* ) 2003 *Phys. Rev. Lett.* **91** 042301
- [13] Rapp R and Wambach J 2000 *Adv. Nucl. Phys.* **25** 1
- [14] Heinz U W and Jacob M 2000 arXiv:nucl-th/0002042
- [15] Karsch F and Laermann E 2003 in Hwa R C and Wang X-N (eds.) *et al Quark gluon plasma* 1, and arXiv:hep-lat/0305025
- [16] Gyulassy M, Vitev I, Wang X-N and Zhang B-W 2003 in Hwa R C and Wang X-N (eds.) *et al Quark gluon plasma* 123, and arXiv:nucl-th/0302077
- [17] Teaney D, Lauret J and Shuryak E V 2001 *Phys. Rev. Lett.* **86** 4783
- [18] Hwa R and Yang C B 2003 *Phys. Rev. C* **67** 034902
- [19] Greco V, Levai P and Ko C M 2003 *Phys. Rev. C* **68** 034904
- [20] Fries R J, Müller B, Nonaka C and Bass S A 2003 *Phys. Rev. C* **68** 044902
- [21] Xu Zhe and Greiner C 2004 arXiv:hep-ph/0406278
- [22] Rapp R and Grandchamp L 2004 *J. Phys. G: Nucl. Phys.* **30** S305
- [23] Drees A 1996 *Nucl. Phys. A* **610** 536c
- [24] McLerran L D and Toimela T 1985 *Phys. Rev. D* **31** 545
- [25] Weldon H A 1990 *Phys. Rev. D* **42** 2384
- [26] Prakash M, Rapp R, Wambach J and Zahed I 2002 *Phys. Rev. C* **65** 034906
- [27] Shuryak E V 1980 *Phys. Rep.* **61** 71
- [28] Asakawa M and Hatsuda T 2003 *Nucl. Phys. A* **715** 863

- [29] Casalderrey-Solana J and Shuryak E V 2004 arXiv:hep-ph/0408178
- [30] Shuryak, E V 1978 *Sov. J. Nucl. Phys.* **28** 408
- [31] Kajantie K and Miettinen H I 1981 *Z. Phys.* **C9** 341
- [32] Kapusta J, Lichard P and Seibert D 1991 *Phys. Rev. D* **44** 2774, erratum 1993 *ibid.* **47** 4171
- [33] Baier R, Nakjagawa H, Niegawa A and Redlich K 1992 *Z. Phys. A* **53** 433
- [34] Arnold P, Moore G D and Yaffe L G 2001 *JHEP* **0112** 009
- [35] Harada M and Yamawaki K 2001 *Phys. Rev. Lett.* **86** 757
- [36] ALEPH Collaboration (Barate R *et al* ) 1998 *Eur. Phys. J. C* **4** 409.
- [37] Rapp R 2003 *Pramana* **60** 675, and arXiv:hep-ph/0201101
- [38] Weinberg S 1967 *Phys. Rev. Lett.* **18** 507
- [39] Kapusta J I and Shuryak E V 1994 *Phys. Rev. D* **46** 4694
- [40] Rapp R, Urban, M, Buballa M and Wambach J 1998 *Phys. Lett. B* **417** 1
- [41] Klingl F, Kaiser N and Weise W 1997 *Nucl. Phys. A* **624** 527
- [42] Leupold S, Peters W and Mosel U 1998 *Nucl. Phys. A* **628** 311
- [43] Steele J V and Zahed I 1999 *Phys. Rev. D* **60** 037502
- [44] Brown G E and Rho M 1991 *Phys. Rev. Lett.* **66** 2720
- [45] Bratkovskaya E L, Cassing W, Rapp R and Wambach J 1998 *Nucl. Phys. A* **634** 168
- [46] Bratkovskaya E L and Ko C M 1999 *Phys. Lett. B* **445** 265
- [47] Shekhter K *et al* 2003 *Phys. Rev. C* **68** 014904
- [48] HADES Collaboration (Salabura P *et al* ) 2004 *Prog. Part. Nucl. Phys* **53** 49
- [49] Rapp R and Wambach J 1999 *Eur. Phys. J. A* **6** 415
- [50] Rapp R, Chanfray G and Wambach J 1997 *Nucl. Phys. A* **617** 472
- [51] NA60 Collaboration (Sonderegger P *et al* ) 2004 *J. Phys. G: Nucl. Phys.* **30** 1027
- [52] Damjanovic S (NA60 Collaboration) 2003 *private communication*
- [53] Rapp R 2001 *Phys. Rev. C* **63** 054907
- [54] Post M and Mosel U 2001 *Nucl. Phys. A* **688** 808
- [55] Riek F and Knoll F 2004 *Nucl. Phys. A* **740** 287
- [56] Martell A T and Ellis P J 2004 *Phys. Rev. C* **69** 065206
- [57] Holt L and Haglin K 2004 *these proceedings*, and arXiv:nucl-th/0409036
- [58] Rapp R and Shuryak E V 2000 *Phys. Lett. B* **473** 13
- [59] Kvasnikova I, Gale C and Srivastava D K 2002 *Phys. Rev. C* **65** 064903
- [60] PHENIX Collaboration (Nagle J *et al*) 2003 *Nucl. Phys. A* **715** 252
- [61] Rapp R 2002 *Phys. Rev. C* **66** 017901
- [62] Averbeck R (PHENIX Collaboration), *private communication*
- [63] Shuryak E V 1997 *Phys. Rev. C* **55** 961
- [64] van Hees H and Rapp R 2004 arXiv:nucl-th/0409026
- [65] Alam J, Sarkar S, Roy P, Hatsuda T and Sinha B 2001 *Ann. Phys., NY* **286** 159
- [66] Peitzmann T and Thoma M 2002 *Phys. Rev.* **364** 175
- [67] Gale C and Haglin K 2003 in Hwa R C and Wang X-N (eds.) *et al Quark gluon plasma* 364, and arXiv:hep-ph/0306098
- [68] Rapp R 2004 *Mod. Phys. Lett. A* **19** 1717, and arXiv:nucl-th/0406016
- [69] Aurenche P, Gelis F, Kobes R and Zaraket H 1998 *Phys. Rev. D* **58** 085003
- [70] Turbide S, Rapp R and Gale C 2004 *Phys. Rev. C* **69** 014903
- [71] Alam J, Roy P and Sarkar S 2003 *Phys. Rev. C* **68** 031901
- [72] Niculescu I *et al* 2000 *Phys. Rev. Lett.* **85** 1182
- [73] WA98 Collaboration (Aggarwal M M *et al*) 2000 *Phys. Rev. Lett.* **85** 3595
- [74] Huovinen P, Ruuskanen P V and Räsänen S S 2002 *Phys. Lett. B* **535** 109
- [75] WA98 Collaboration (Aggarwal M M *et al*) 2004 *Phys. Rev. Lett.* **93** 022301
- [76] Turbide S, Rapp R and Gale C *work in progress*
- [77] PHENIX Collaboration (Frantz J *et al* ) 2004 *J. Phys. G: Nucl. Phys.* **30** S1003
- [78] Räsänen S S 2003 *Nucl. Phys. A* **715** 717